Supplemental Material

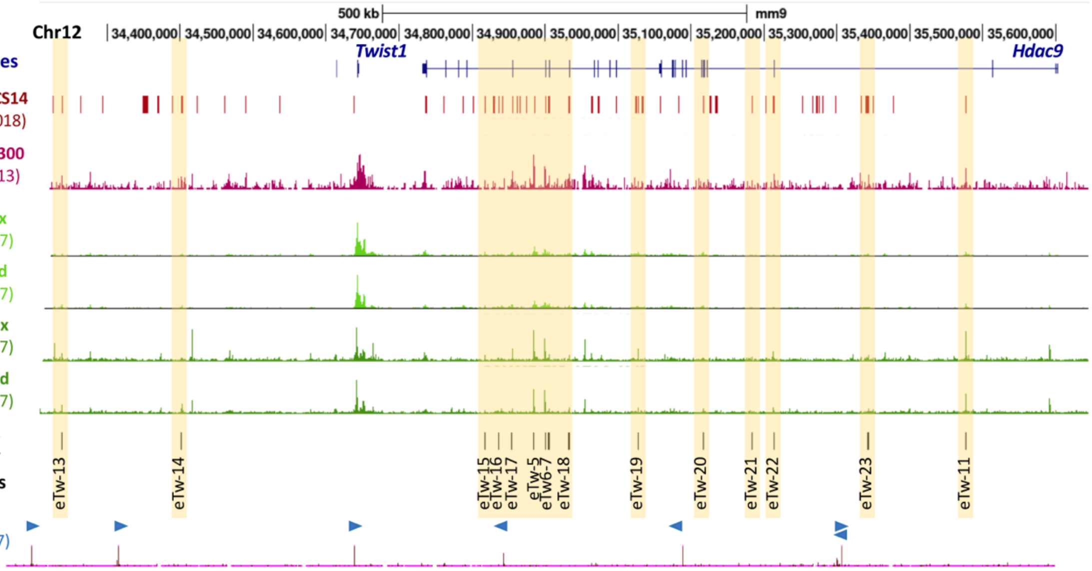

Supplementary Figure 1. 15 enhancer candidates at the *Twist1-Hdac9* locus. UCSC genome browser tracks of enhancer-associated marks from early human embryonic craniofacial tissues (stages CS13-CS14) (Wilderman, 2018); p300 ChIP-seq from mouse E11.5 craniofacial tissues (Attanasio et al., 2013); H3K27ac ChIP-seq and ATAC-seq from the maxilla (Mx) and mandibula (Md) E11.5 mouse embryos (Minoux et al. 2017). Selected enhancer candidates are marked by a yellow rectangle. CTCF ChIP-seq from mouse E11.5 limb bud (Andrey et al., 2017). Blue triangles marked bound CTCF site and its directionality.

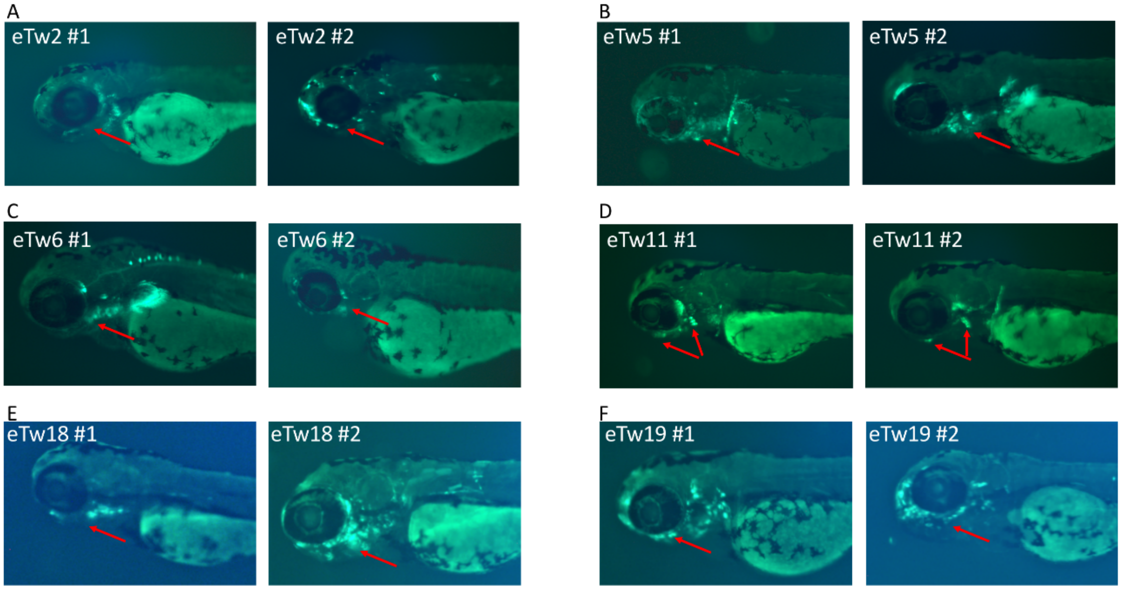

Supplementary Figure 2. **Functional craniofacial enhancers in the HDAC9-TWIST1 locus characterized using zebrafish. (A)** eTw-2 drives GFP expression in branchial arches 1-2. **(B)** eTw-5 drives GFP expression in the nasal pit and branchial arches 1-7. **(C)** eTw-6 drives GFP expression in the branchial arches 1-2. **(D)** eTw-11 drives GFP expression in the branchial arches 3-7. **(E)** eTw-18 drives GFP expression in the pharyngeal arches. **(F)** eTw-19 drives GFP expression in the mandibular, nasal pit, and branchial arches (red arrows). The GFP expression drove by each enhancer (red arrows) is represented by two different fish at 72hpf.

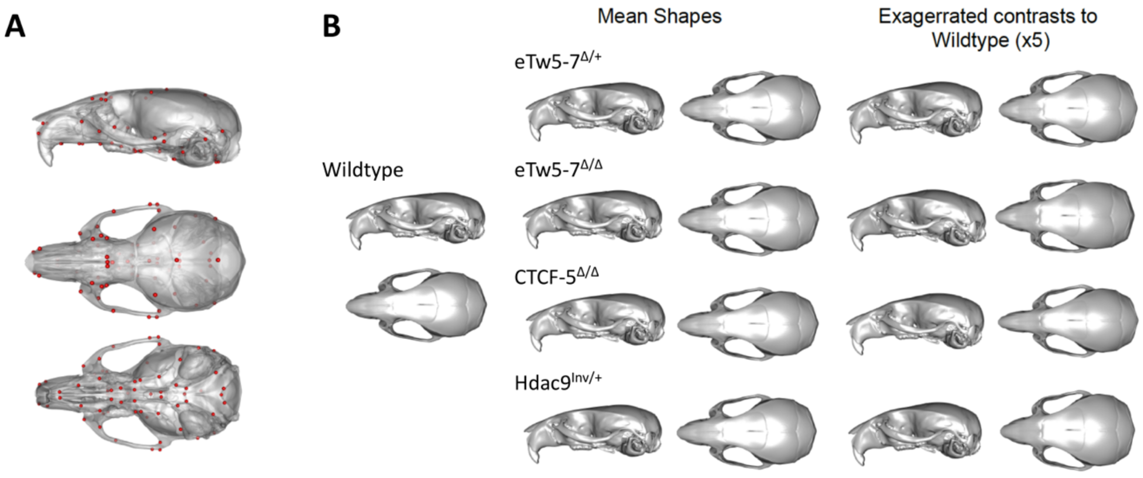

Supplementary Figure 3. **Skull size and shape of mouse models for *Twist1* regulatory elements (A)** 68 standardized skeletal landmarks (red dots) used to quantify 3D craniofacial form (shape and size) from micro-CT scans. **(B)** 3D morphs from micro-CT data of eTw5-7$^{\Delta/\Delta}$, eTw5-7$^{\Delta/+}$, CTCF-5$^{\Delta/\Delta,}$ and Hdac9$^{INV/+}$ mice compared to wild-type show the differences in mean skull shape that also demonstrated by exaggerated contrasts of each model to wildtype (×5).

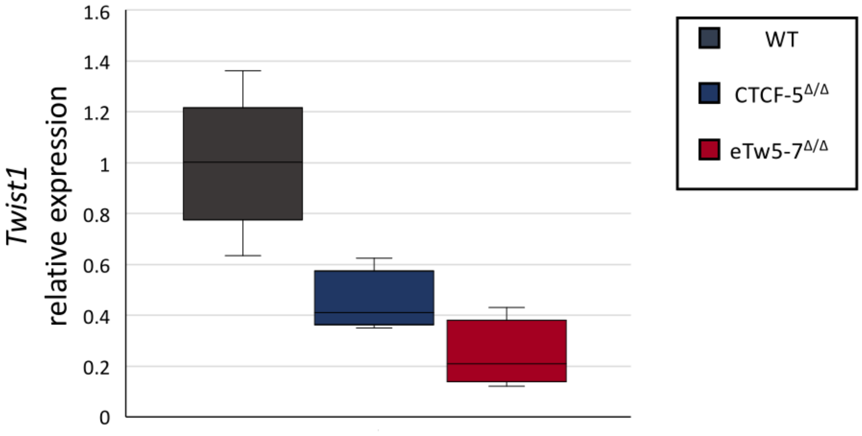

Supplementary Figure 4: Twist1 expression levels in mouse E11.5 branchial arches. mRNA expression levels of Twist1 in wildtype, CTCF-$5^{\Delta/\Delta}$ and eTw5-$7^{\Delta/\Delta}$ are normalized to beta-actin expression ($p<0.05$, Student's *t*-test).

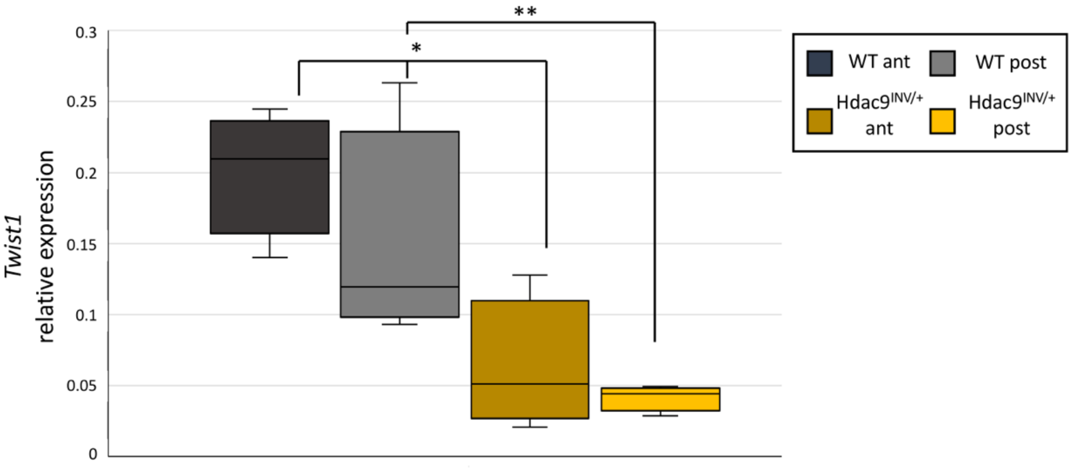

Supplementary Figure 5: *Twist1* expression in E11.5 HL of Hdac9$^{INV/+}$ and WT mouse embryos. mRNA expression levels of Twist1 are normalized to beta-actin expression ($p<0.05$, Student's *t*-test).

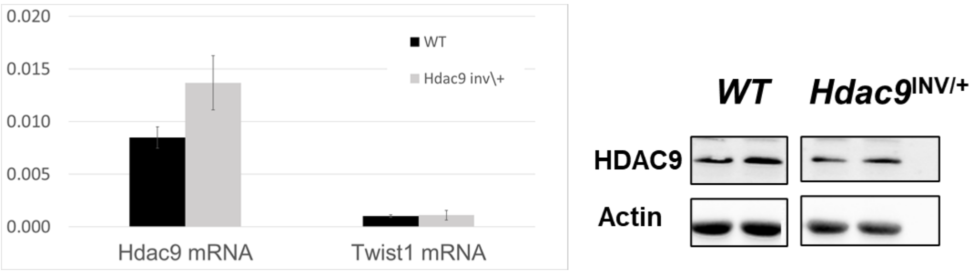

Supplementary Figure 6: Hdac9 expression levels in adult mouse brain. **(A)** mRNA expression levels of Hdac9 and Twist1 of adult mouse brains of wild type and *Hdac9*$^{\text{INV/+}}$**.** **(B)** Western blot analysis of Hdac9 protein level in adult mouse brains of wild type and *Hdac9*$^{\text{INV/+}}$ (Anti-Hdac9; ab59718).

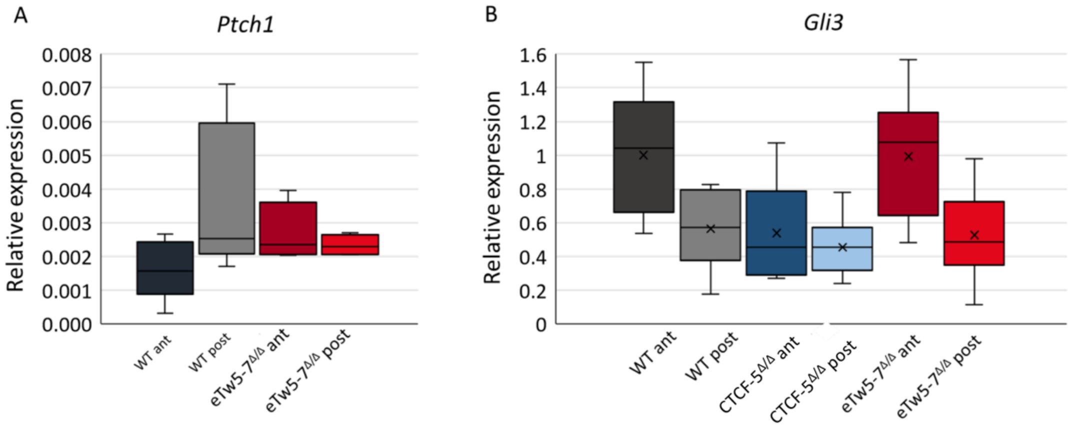

Supplementary Figure 7: Expression pattern of Shh pathway genes. **(A)** mRNA expression levels of *Ptch1* in HL of E11.5 WT and eTw5-7$^{\Delta/\Delta}$ mouse embryos. **(B)** mRNA expression levels of *Gli3* in HL of E11.5 WT, eTw5-7$^{\Delta/\Delta}$ and CTCF-5$^{\Delta/\Delta}$ mouse embryos.

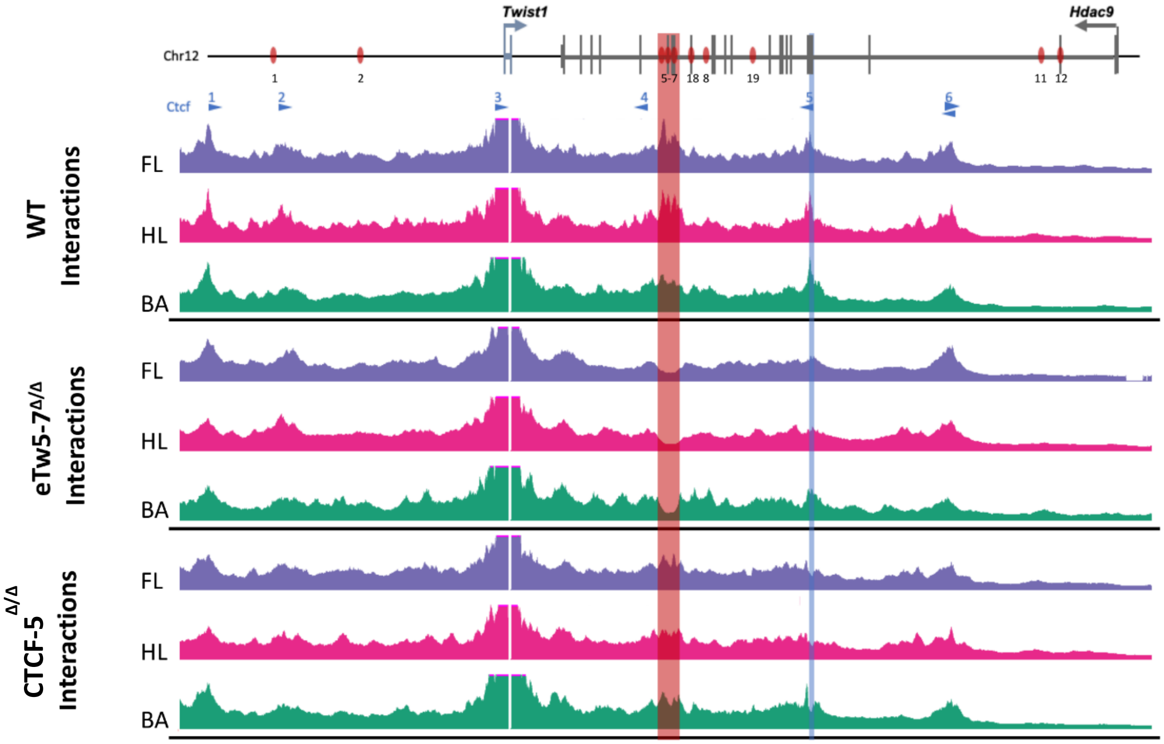

Supplementary Figure 8: UMI-4C data representing chromatin looping in the Hdac9-Twist1 locus. UMI-4C tracks of merged from two biological replicates) of WT E11.5 forelimb (FL), Hindlimb (HL), and Branchial arch (BA) demonstrate that Twist1 interaction patterns are largely conserved between limb buds and branchial arch. The Twist1 promoter serves as a viewpoint. Targeted eTw5-7 and CTCF-5 regions are indicated by red and blue dash rectangles, respectively.

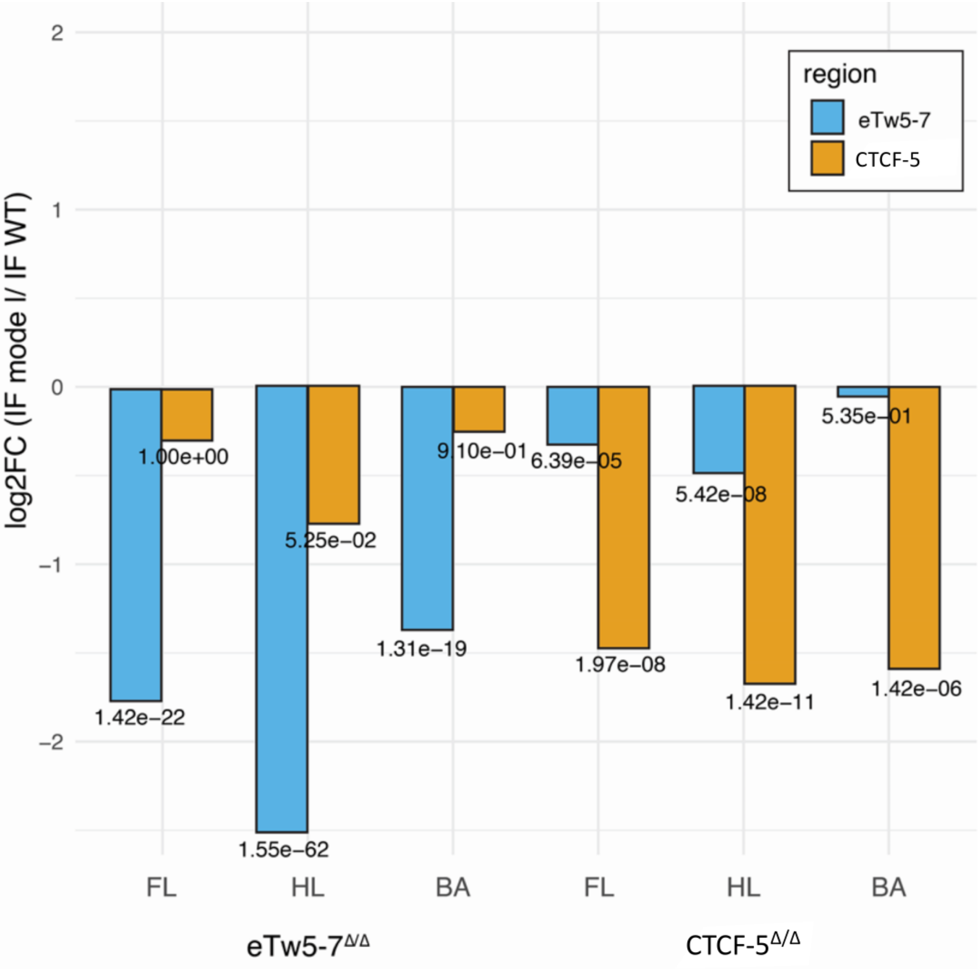

Supplementary Figure 9: Differential interaction frequencies of eTw5-7 and CTCF-5 site regions with Twist1 promoter in our mouse models. Log2 fold changes (FC) of the interaction frequency (IF) of Twist1 promoter and eTw5-7 region or CTCF-5 region in wildtype versus eTw5-7$^{\Delta/\Delta}$ or CTCF-5$^{\Delta/\Delta}$ mice. Log2 fold changes of interaction frequencies from UMI-4C are presented for forelimb (FL), hindlimb (HL), branchial arch (BA). Statistical significance (P-value) of differential interactions was tested for these two loci (eTw5-7: Chr12:34883878-34906858, CTCF-5: Chr12:35116684-35117991, mm9) using a Chi-square test within the UMI-4C R package (p4cIntervalsMean function).

Supplementary Movie 1: Centroid size and shape of eTw5-7$^{\Delta/\Delta}$ (superior view). Here, the vector of landmark by landmark shape differences is used to quantify the difference between each genotype and the wildtype mean. Movies S1-S6 show an exaggeration (from 0-10×) of this shape difference vector to visualize the anatomical direction and distribution of shape effects by genotype.

Supplementary Movie 2: Centroid size and shape of eTw5-7$^{\Delta/\Delta}$ (side view).

Supplementary Movie 3: Centroid size and shape of CTCF-5$^{\Delta/\Delta}$ (superior view).

Supplementary Movie 4: Centroid size and shape of CTCF-5$^{\Delta/\Delta}$ (side view).

Supplementary Movie 5: Centroid size and shape of Hdac9$^{INV/+}$ (superior view).

Supplementary Movie 6: Centroid size and shape of Hdac9$^{INV/+}$ (side view).